Effect of Hydrogenated Cardanol on the Structure of Model Membranes Studied by EPR and NMR

ARTICLE *in* LANGMUIR · AUGUST 2013

Impact Factor: 4.46 · DOI: 10.1021/la402008n · Source: PubMed

6 AUTHORS, INCLUDING:

Stefania Santeusanio
Università degli Studi di Urbino "Carlo Bo"
91 PUBLICATIONS **839** CITATIONS
SEE PROFILE

Roberta Majer
Università degli Studi di Urbino "Carlo Bo"
3 PUBLICATIONS **7** CITATIONS
SEE PROFILE

Michela Cangiotti
Università degli Studi di Urbino "Carlo Bo"
45 PUBLICATIONS **335** CITATIONS
SEE PROFILE

Alberto Fattori
Università degli Studi di Urbino "Carlo Bo"
12 PUBLICATIONS **95** CITATIONS
SEE PROFILE

Langmuir

Article

pubs.acs.org/Langmuir

Effect of Hydrogenated Cardanol on the Structure of Model Membranes Studied by EPR and NMR

Stefania Santeusanio,*[,†] Orazio Antonio Attanasi,[†] Roberta Majer,[†] Michela Cangiotti,[‡] Alberto Fattori,[‡] and Maria Francesca Ottaviani*[,‡]

[†]Department of Biomolecular Sciences, University of Urbino, Via Maggetti 24, 61029 Urbino, Italy

[‡]Department of Earth, Life and Environment Sciences, University of Urbino, Località Crocicchia, 61029 Urbino, Italy

Supporting Information

ABSTRACT: Hydrogenated cardanol (HC) is known to act as an antiobesity, promising antioxidant, and eco-friendly brominating agent. In this respect, it is important to find the way to transport and protect HC into the body; a micellar structure works as the simplest membrane model and may be considered a suitable biocarrier for HC. Therefore, it is useful to analyze the impact of HC in the micellar structure and properties. This study reports a computer aided electron paramagnetic resonance (EPR) and ^{1}H NMR investigation of structural variations of cetyltrimetylammonium bromide (CTAB) micelles upon insertion of HC at different concentrations and pH variations. Surfactant spin probes inserted in the micelles allowed us to get information on the structure and dynamics of the micelles and the interactions between HC and CTAB. The formation of highly packed HC-CTAB mixed micelles were favored by the occurrence of both hydrophobic (chain−chain) and hydrophilic (between the polar and charged lipid heads) interactions. These interactions were enhanced by neutralization of the acidic HC heads. Different HC localizations into the micelles and micellar structures were identified by changing HC/CTAB relative concentrations and pH. The increase in HC concentration generated mixed micelles characterized by an increased surfactant packing. These results suggested a rod-like shape of the mixed micelles. The increase in pH promoted the insertion of deprotonated HC into less packed micelles, favored by the electrostatic head−head interactions between CTAB and deprotonated-HC surfactants.

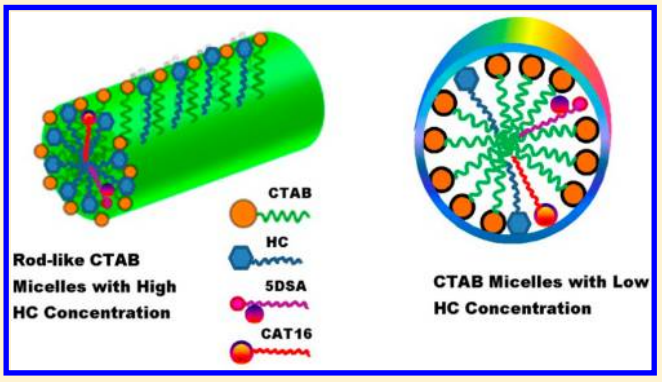

1. INTRODUCTION

Processes that convert bio- or industrial waste into value-added chemicals such as functional materials, have been proven to be an alternative platform to build the concept of biorefinery.[1,2] In this context, a model case is well represented by the cashew nutshell liquid (CNSL), which is the oil derived from the spongy mesocarp of cashew nut shell (*Anacardium occidentale* L.) that is used as byproduct in the food processing of the nuts.[3−5]

This oil has a high potential usefulness in chemical reactions to allow fine chemicals with a wide range of applications.[3−7] In general, the initial composition of natural CNSL is a mixture of anacardic acid (70%), which is thermolabile and converts to cardanol (naturally present at 18%), cardol (5%), and other phenols (7%).[8,9]

Distilled cardanol results in a rich mixture of phenolic lipids,[10−12] which possess exciting functional flexibility that could lead to generating a variety of soft nanomaterials such as nanotubes, nanofibers and gels.[5,13] This is due to two main structural and chemical features: the reactive phenolic −OH group and the *meta* alkyl chain with nonisoprenoic *cis* double bonds similar to linear alkyl benzenes.

The complete hydrogenation of cardanol leads to the mono phenol hydrogenated cardanol (HC: chemical formula reported in Figure 1), that is known to act as antiobesity,[14] promising antioxidant,[15] and eco-friendly brominating agent.[16]

The interest in this compound by Science and Industry is related to the low cost production of HC from CNSL in view to offer a biobased material with surfactant-like properties.

Solubilization of poorly to moderately water-soluble components forms the basis for the application of concentrated surfactant products. In addition, micellar solubilization has been investigated as a possible formulation strategy for poorly water-soluble drugs,[17] and it has been proposed as an useful tool in soil remediation.[18]

Due to its amphiphilic nature, HC could be easily incorporated into a micelle, which gives the simplest membrane model, suitable to work as HC protector and carrier in water solution. It is of significant interest to find the way to accumulate and transport HC in solution to provide bioavailability of this compound, and on the same time, verify

Received: May 26, 2013
Revised: July 9, 2013
Published: August 5, 2013

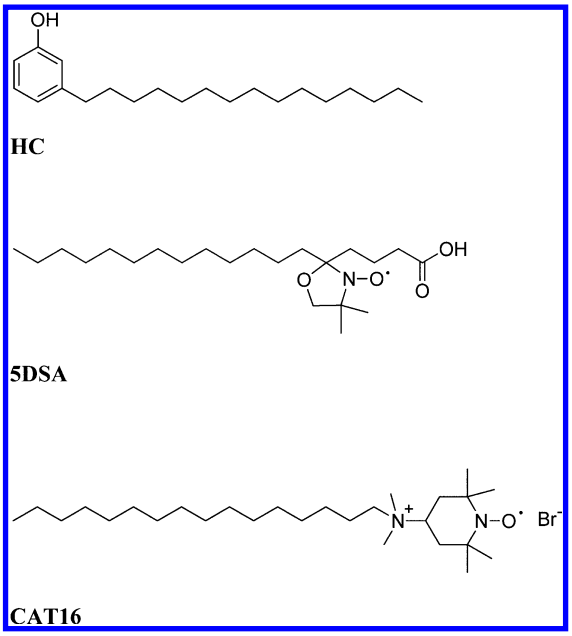

Figure 1. Chemical formulas of HC, 5DSA, and CAT16.

the bioimpact of HC onto the structure of surfactant aggregates mimicking the cell membrane. Therefore, we investigated the structural variations of micelles obtained from cetyltrimetyl ammonium bromide (CTAB) at concentration 0.1 M upon insertion of HC at different concentrations by means of electron paramagnetic resonance (EPR) and ^{1}H NMR spectroscopies. CTAB was selected because we expected a further stabilization of HC into CTAB micelles due to interactions between the OH group of HC and the positively charged head of CTAB. Further measurements were carried out using egg yolk lecithin liposomes as a more reliable model membrane. Nevertheless the results, also discussed in the present report, were less informative than the ones obtained using CTAB micelles. Two different surfactant spin probes were selected for EPR studies, both able to insert into the micelles and considered well representative of the behavior of the surfactants constituting the micelles,[19] that were: (a) the hydrophobic spin probe 5-doxylstearic acid (5DSA: chemical formula reported in Figure 1), which has the paramagnetic group in the position 5 of the stearic chain and therefore is able to monitor structural variations of the CTAB micelles in the lipid region just below the polar heads, which is the most organized micelle region; (b) the hydrophilic (water-soluble) spin probe 4-cetyl-dimethylammonium-2,2,6,6,-tetramethylpiperidine *N*-oxyl bromide (CAT16: chemical formula reported in Figure 1); in this case, the paramagnetic group is positioned at the micelle surface and has the same charge and similar structure as the CTAB head. The use of spin probes already demonstrated to provide very useful information about the structure of surfactant aggregates by the use of a computer aided analysis of the EPR line shape.[19−26]

2. EXPERIMENTAL SECTION

2.1. Materials. CTAB, 5DSA and sodium hydroxide pellets (97+% ACS reagent) were purchased from Sigma Aldrich. HC was prepared in our laboratory following the procedure already reported in the literature.[15,16] CAT16 spin probe was kindly provided by Dr. X. Lei, Columbia University, New York. Lecithin from egg yolk (L-R Lecithin) was purchased from Fluka. Egg yolk lecithin is a natural and low cost phospholipid. It consists of a mixture of phospholipids with different chain lengths and insaturations on the fatty acyl chain. The acyl chains will be noted C*n*:*m* where *n* is the number of carbon atoms of the chain and *m* the number of insaturations in the chain. Egg yolk lecithin is composed of 1.8% myristic acid (C14:0), 36.5% palmitic acid (C16:0), 14% stearic acid (C18:0), 4.3% palmitoleic acid (C16:1), 30% oleic acid (C18:1), 13.5% linoleic acid (C18:2). Multilamellar liposomes were obtained by drying a chloroform solution of lecithin under a nitrogen stream for 30 min so that a thin film is formed at the bottom of a glass tube and then hydrating the film by adding water and vortexing the dispersion for 15 s. The gel−liquid crystalline transition temperature T_c of egg yolk lecithin is −15/−17 °C. The liposome preparation was performed at room temperature.

Doubly distilled and purified water (Millipore System) was used in all EPR measurements. Deuterium oxide (99.9 atom % D) was obtained from Cambridge isotope laboratories and used as aqueous phase for ^{1}H NMR measurements.

2.2. Sample Preparation. *2.2.1. Preparation of Samples for EPR Analysis.* The concentration of the probes in water was 0.5 mM, which is low enough to guarantee a low perturbation. To a solution of CTAB (0.1 M) in water, HC was added at different concentrations: 0.01 M, 0.05 M, 0.1 and 0.2 M in order to obtain CTAB:HC ratios of 10:1, 2:1, 1:1 and 1:2, respectively. The pH of the solution was increased by adding NaOH solution at concentration 0.002 and 0.012 M to obtain deprotonation of the OH group of HC. The pH measured for the solution decreased by adding increasing amounts of HC (from 6.8 with HC 0.05 M, to 6.5 with HC 0.1), but it also increased to 7.5 and 8.4, for HC 0.05 M, by adding NaOH at concentrations 0.002 and 0.012 M, respectively.

A single sample ready for the EPR analysis contains the probe (CAT16 or 5DSA), CTAB and HC mixed in different concentrations. The samples with the spin-probe were made adding the CTAB or lecithin aggregates solution to vials containing the proper amount of the spin probe (final concentration 0.5 mM of the spin probe and 0.1 M of CTAB or lecithin) using double distilled (Millipore) water. The probe-surfactant solutions were left equilibrating for a few hours until we did not see any more variations in the EPR spectra. Different amounts of HC were added to the CTAB or lecithin solutions before adding the probe in order to obtain different HC final concentrations (HC 0.01 M, 0.05 M, 0.1 M, and 0.2 M). The HC + CTAB or lecithin solutions were stirred for equilibration for 2 h. After stirring, the solutions were added to the probe solutions as described above. 100 μL of the solutions were inserted into the EPR tube for spectral analysis. For pH variations, NaOH was added to the CTAB or lecithin solutions in the absence and presence of different HC amounts and in the presence of the spin probe to obtain the final NaOH concentrations of 0.002 and 0.012 M.

2.2.2. Preparation of Samples for NMR Analysis. To investigate the interaction between HC and CTAB micelle, as in the EPR experiments, the CTAB concentration was fixed at 0.1 M and HC concentration varied to be 0.005 M, 0.01 M, 0.05 M. To investigate the influence of pH on HC sorption in cationic CTAB micellar solutions, a mixture of 0.1 M CTAB and 0.01 M of HC in D_2O was prepared in the absence and presence of NaOH at concentrations of 0.002 and 0.012 M. In order to minimize temperature effects (room temperature at about 298 K), all the spectra were recorded in one series.

The methodology for the preparation of CTAB solutions for NMR analysis was the same as for EPR analysis.

2.3. Methods. EPR spectra were recorded with a EMX-Bruker spectrometer operating at X band (9.5 GHz) and interfaced with a PC (software from Bruker for handling and recording the EPR spectra). The temperature was controlled with a Bruker ST3000 variable temperature assembly cooled with liquid nitrogen. The reproducibility was verified by repeating each experiment at least three different times. The EPR spectra were recorded at 298 K.

^{1}H NMR spectra were recorded on a Varian 400 MHz apparatus in D_2O solution at 298 K. In all spectra, the HOD peak was assigned at 4.79 ppm according the instrument manual and used as the reference peak.

dx.doi.org/10.1021/la402008n | *Langmuir* 2013, 29, 11118−11126

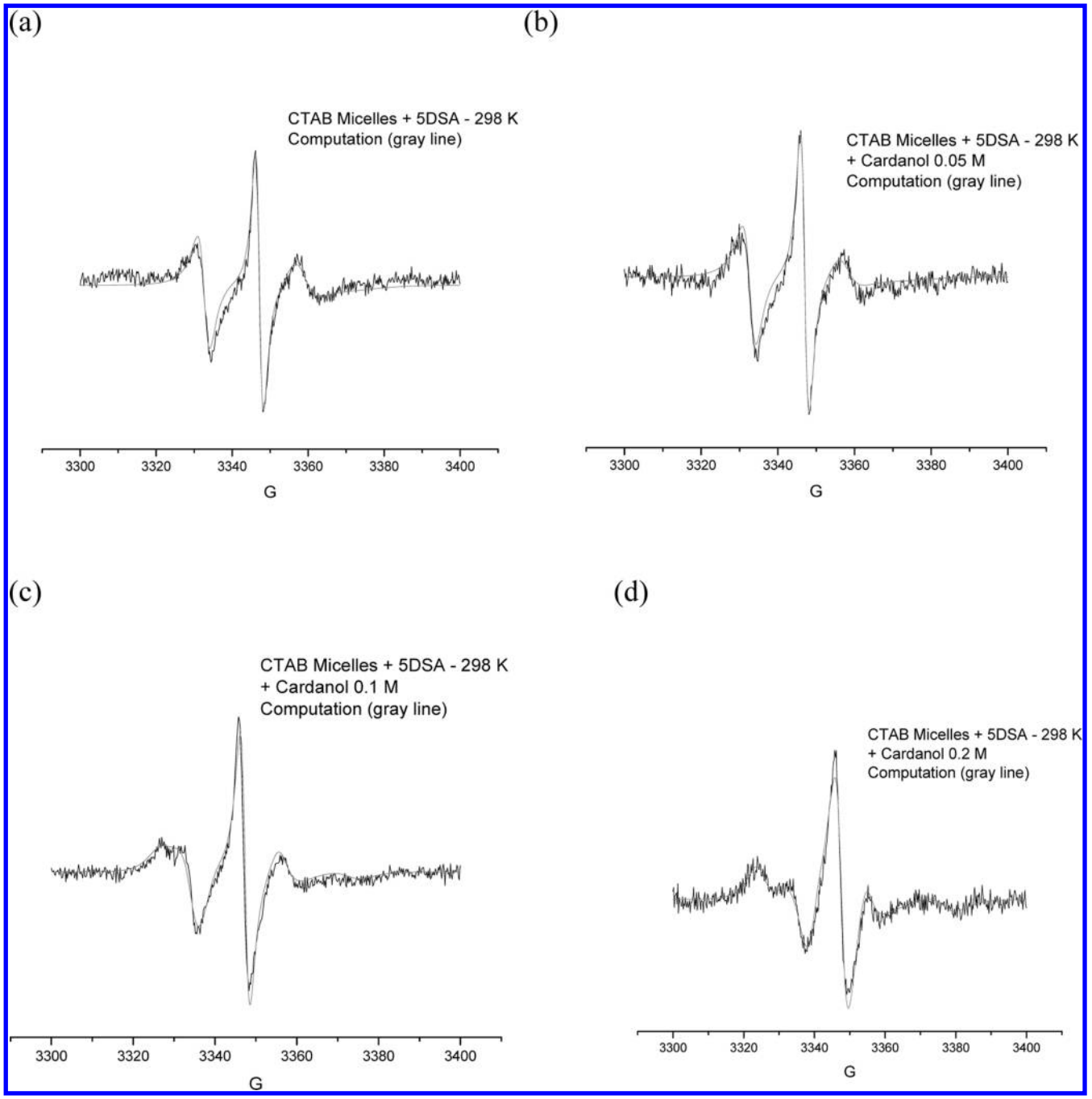

Figure 2. Experimental (298 K) and computed EPR spectra of water solutions of CTAB (0.1 M) micelles containing 5DSA (0.5 mM) and different HC concentrations: 0 M (a), 0.05 M (b), 0.1 M (c), and 0.2 M (d).

2.4. Computation of the EPR Spectra. The EPR spectra were analyzed by means of the program by Budil and Freed[27] to extract parameters informative on the environmental polarity (the hyperfine coupling constant for the coupling between the electron spin and the nitrogen nuclear spin, $\langle A \rangle$) and the mobility (the correlation time for the rotational diffusional motion, τ) of the probe. In the 5DSA case with lecithin liposomes we also had to take into account an order parameter due to a "palisade" structuration of the lipid bilayer. In the CAT16 case, the spectra were constituted by two components due to the distribution of the probes in two different environments. A subtraction procedure between spectra, which were related to different experimental conditions, allowed us to extract the two components to quantify them in different relative percentages and to compute both of them.

The accuracy for all the parameters in the EPR analysis was between 2 and 3%, based on the fitting between the experimental and the computed line shapes, slightly increasing if line broadening occurs.

3. RESULTS AND DISCUSSION

3.1. EPR Analysis. Figure 2 shows the experimental (298 K) and computed spectra of CTAB (0.1 M) water solutions micelles containing 5DSA (0.5 mM) and different HC concentrations. The main parameters of computation $\langle A \rangle$ and τ, are shown in Table 1a.

We clearly see in Table 1a that $\langle A \rangle$ decreases while τ increases by adding HC. The decrease in polarity monitored by the decrease of $\langle A \rangle$ is small, but not negligible, and takes place mainly from 0 to 0.05 M of HC. Conversely, the decrease in

dx.doi.org/10.1021/la402008n | Langmuir 2013, 29, 11118−11126

Table 1. Main Computation Parameters ($\langle A \rangle$, τ and Relative %) of EPR Spectra of CTAB (0.1 M) Solutions in the Absence and Presence of HC and/or NaOH at Different Concentrations

(a) 5DSA (0.5 mM)		
HC [M]	$\langle A \rangle$ (G)	τ (ns)
0	15.00	3.18
0.01	14.95	3.30
0.05	14.80	3.50
0.1	14.80	6.50
0.2	14.80	8.75

(b) CAT16 (0.5 mM)					
HC [M]	NaOH [M]	$\langle A \rangle$ (G) interacting	τ (ns) interacting	% free component	$\langle A \rangle$ (G) free component
0	0	15.3	1.3	80	16.84
0	0.002	16	1.49	44	16.89
0	0.012	16	1.49	44	16.92
0.01	0	15.94	1.73	50	16.9
0.01	0.002	15.99	1.78	48	17.24
0.01	0.012	16.14	1.7	48	16.98
0.05	0	15.93	2.1	65	16.89
0.05	0.002	15.95	2.2	60	16.99
0.05	0.012	15.99	2.3	60	16.93
0.1	0	16.15	2.79	80	16.87
0.1	0.002	16.47	2.83	75	16.87
0.1	0.012	16.38	2.83	75	16.87

mobility monitored by the increase in τ is significant, mainly from 0.05 to 0.1 M and to 0.2 M. The small decrease in polarity indicates that the radical group is already in the low polar micellar core and HC poorly changes the polarity of this environment. The decrease in mobility indicates that HC modifies the structure of the aggregates and originates a more compact, but not ordered (no ordered parameter is needed in the computation), structure. Such variations are well ascribed, on the basis of similar variations in similarly structured systems,[19,24−26] to the formation of mixed CTAB/HC micellar aggregates, with a more "rod-like" shape. Such elongated shape is expected due to both the different sizes of HC and CTAB, and the interactions occurring at the polar surface between CTAB and HC heads. Since 5DSA monitors the interactions occurring into the lipid layer in the region close to the lipid/water interface, hydrophobic interactions are also playing a significant role in modifying the surfactant organization, and, consequently, the EPR line shape. Interestingly, the addition of NaOH at concentrations 0.002 and 0.012 M almost does not modify the EPR line shape. An explanation of this result may be found in the location of the radical group internally the micelles, where the deprotonation of the −OH groups of HC at higher pH poorly affects the doxyl group environment and mobility. We have also to consider that 5DSA has a pK_a close to neutrality.[28] This means that it is largely deprotonated even in the presence of HC, and, when HC also deprotonates, the two negative moieties stay far from each other. Furthermore, the hydrophobic chain of 5DSA goes into the packed lipid layer to escape from the charged interface. The results obtained with the positively charged CAT16 probe (*vide infra*) support this hypothesis.

We also tried a different model membrane that is liposomes constituted by egg yolk lecithin (0.1 M). As shown in Figure S1 (Supporting Information), the addition of HC at concentrations 0.01 and 0.1 M induces a small but not negligible variation of 5DSA mobility. Indeed τ increases from 6.05 ns in the absence of HC, to 6.30 and 6.65 ns in the presence of 0.01 and 0.1 M of HC, respectively. Contemporaneously, both polarity, measured by $\langle A \rangle$ = 14 G, and the order parameter, measured by S = 0.38, do not change. These results show that the liposome structure is poorly affected by HC. However, the higher the HC concentration, the stronger the interactions are in the lipid layer in vicinity of the heads, where the doxyl group of 5DSA is positioned.

A different and in some respect more interesting behavior is revealed by CAT16 as a probe inserted into the CTAB micelles. Figure 3 shows (a) the experimental EPR spectrum at 298 K of a water solution containing CTAB (0.1 M) micelles + CAT16 (0.5 mM) + HC 0.05 M. This spectrum is selected as an example to underline (through the use of arrows) the presence of two spectral components for the CAT16 probe. They are termed "interacting" and "free" on the basis of the parameters extracted from computation (see below); (b) the experimental (298 K) and computed spectra of water solutions of CAT16 (0.5 mM). This last spectrum represents the "free" component which is also identified, with some modifications, in the spectrum in Figure 4a.

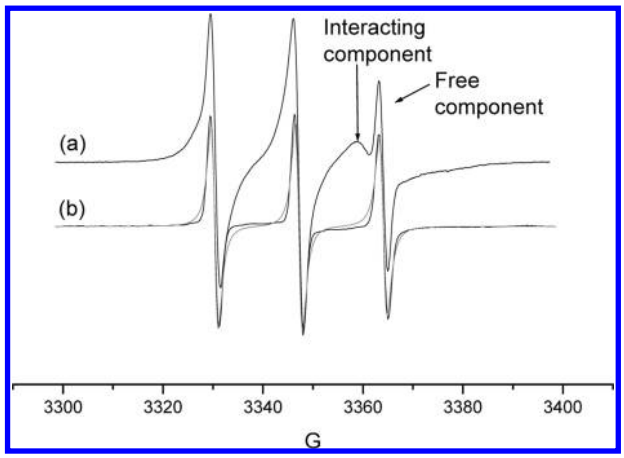

Figure 3. (a) Experimental (298 K) EPR spectrum of CTAB (0.1 M) micellar solution + CAT16 (0.5 mM) + Cardanol 0.05 M. (b) Experimental (298 K) and computed EPR spectra of CAT16 (0.5 mM) water solution. Computation (gray line): $\langle A \rangle$ = $\langle A \rangle$16.87 G; τ = 0.07 ns.

This signal arises from radicals which are free to move in water solution, and was computed with a low τ (0.07 ns, high mobility) and a high $\langle A \rangle$ (16.87 G, high polarity). We found that almost all the spectra of CAT16 in CTAB micellar solution in the absence and presence of HC show a free component whose relative percentage changes as a function of the different experimental conditions. To extract the two components, interacting and free, we tried to subtract the experimental spectra from one other. The spectra subtraction was made more difficult by the fact that both the components, interacting and free, change from one system to another. The main reason for the spectra subtraction is the extraction of the interacting component, which arises from probes embedded into the condensed micellar phase. In order to subtract the free component from the overall EPR signal, we used the computed free component shown in Figure 3b for all spectral subtractions by changing the peak-to-peak distance which gives the polarity parameter $\langle A \rangle$.

dx.doi.org/10.1021/la402008n | *Langmuir* 2013, 29, 11118−11126

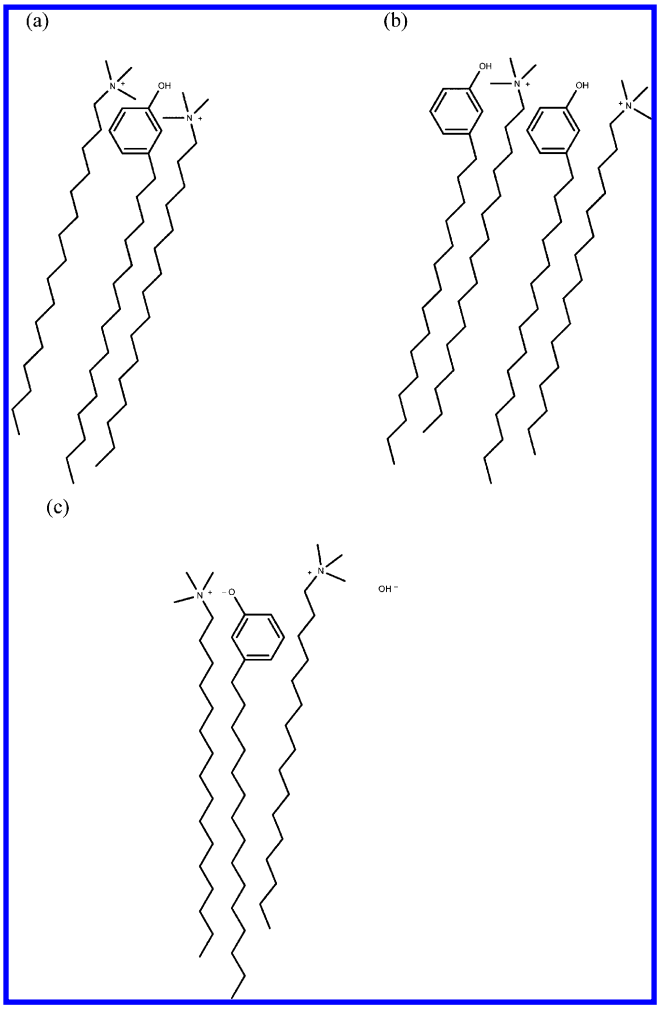

Figure 4. Scheme of the local organization of CTAB and HC surfactants at (a) the lower HC concentrations (up to 0.01 M), (b) the higher HC concentrations (0.05−0.1 M), and (c) a higher pH after addition of NaOH (0.002−0.012 M).

This approximation produces some "imperfections" in the experimental interacting component indicated in the top spectrum in Figure S2 (SI). These imperfections almost equivalently affect all the computations of the interacting components in the different experimental conditions. As a consequence, the accuracy for the parameters obtained from computation, decreases from 2% to 5%, but the trends in the parameter variations result almost unaffected by the presence of such imperfections. Table 1b reports the main computation parameters ($\langle A \rangle$, which measures the polarity, τ which measures the strength of interactions, and the relative percentage %, which measures the permeability and packing (surfactant density) of the aggregate structure) related to the "interacting" components obtained after subtraction of the "free" component, for CTAB (0.1 M) micelles containing CAT16 (0.5 mM) in the absence and presence of different HC and NaOH concentrations (0.01, 0.05, 0.1, and 0.2 M, for HC, and 0.002, and 0.012 M, for NaOH). The $\langle A \rangle$ values of the "free" components are also listed in Table 1b. The computations of the "interacting" components are shown in Figure S2 (SI).

Before discussing the EPR results, it is useful to clarify the protonation conditions of the system in the different experimental conditions. First of all, it is known that the pK_a of alkylated phenol is >10 and increases by increasing the alkyl chain length.[29] Therefore HC is an acidic compound, but much less acidic than phenol. Indeed, the addition of HC decreases the pH of CTAB solutions from 7.76 to 7.6 (HC 0.01 M), 6.8 (HC 0.05 M), and 6.5 (HC 0.1 M). So, a partial deprotonation of HC occurs in CTAB solution, but the deprotonation is lower at higher HC concentrations. We have to remember that HC in water is almost completely insoluble in all the pH range, and therefore we could not analyze the deprotonation behavior in water. However, it is also necessary to take into account the surface pH. As CTAB micelles are cationic, hydroxyl ions are attracted, which causes the pH at the CTAB micellar surface to be much higher than the bulk. As such, solubilized HC could be already dissociated at neutral (bulk) pH.

The percentage of free component strongly decreases (from 80% to 50%) by adding the smallest amount of HC (0.01 M). This is because HC drives the spin probe (and CTAB) inside the micelles and increases the interactions (measured by the increase of τ) at the micellar surface where the polarity (measured by $\langle A \rangle$) is higher. This result means that HC at this concentration increases the number of surfactants constituting the micelles by changing the micellar structure (as described above, a rod-like conformation is suggested on the basis of previous results from similar systems). The increased interaction supports the occurrence of hydrophilic interactions between the polar HC heads and the charged CTAB heads (already hypothesized from 5DSA results). These interactions may be even stronger if HC partially dissociated upon sorption. This introduces a decreased electrostatic repulsion that is also responsible for the decrease in free component percentage. Figure 4a provides a sketch of the proposed organization of the CTAB and HC surfactants in the mixed micelles at low (0.01 M) HC concentration.

By increasing the amount of HC from 0.01 to 0.05 M and to 0.1 M, the percentage of free component increased from 50%, to 65% and to 80% (0.2 M is not reported since the interacting component becomes hardly recognizable). This indicates that a high concentration of HC works as a barrier shielding the internalization of the free surfactants. In order to explain this behavior, we have to consider that the mobility decreases while the polarity increases with the increase in HC concentration. All these results are well explained by an internalization of HC into a mixed-micellar rod-like structure. The HC internalization, which was mimicked by the 5DSA internalization, promotes the approaching of the positively charged CTAB or CAT16 heads to the OH groups of HC: this decreases the CAT16 head mobility, increases its polarity, and impedes further internalization of the charged surfactants, also because the surfactant structure is less packed due to the steric hindrance of the aromatic group into the aggregates. Figure 4b provides a sketch of the proposed organization of the CTAB and HC surfactants in the mixed micelles at the higher (0.05−0.1 M) HC concentrations.

The EPR analysis showed that the percentage of free component is higher in the absence than in the presence of NaOH (higher pH). This effect, which is more pronounced in the absence of HC, is the result of different simultaneous effects: (i) the increased ionicity of the solution, which decreases the solubility of the surfactants in water; this is due to the ions repulsion toward the hydrophobic chain that increases the surfactant solubility into the micelles; the increased ionicity also causes the increase in $\langle A \rangle$ for the free component; (ii) the decrease of the positive charge at the

dx.doi.org/10.1021/la402008n | Langmuir 2013, 29, 11118−11126

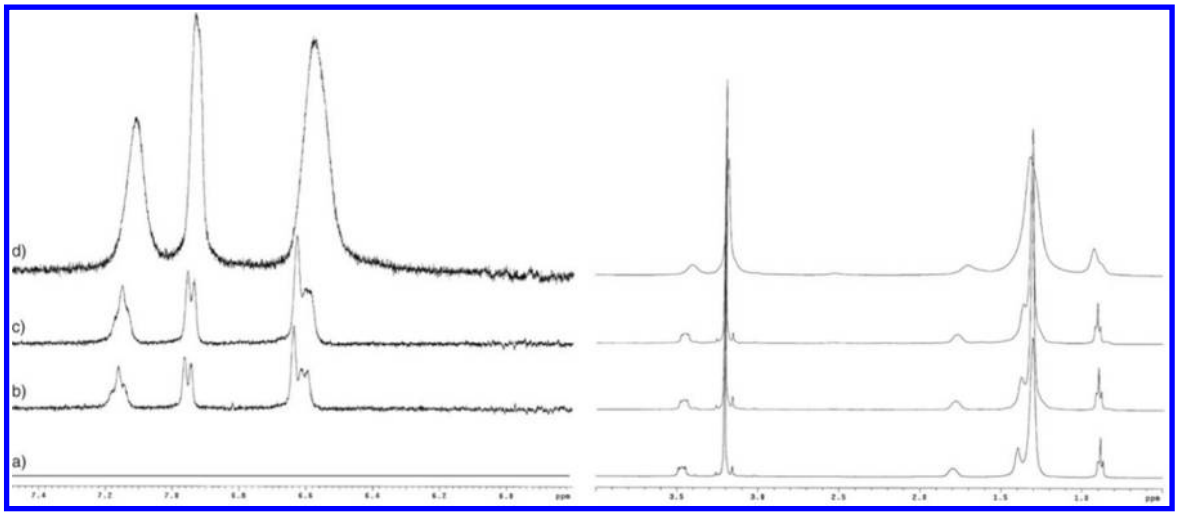

Figure 5. ^{1}H NMR spectra of (a) 0.1 M CTAB, (b) 0.005 M HC and 0.1 M CTAB, (c) 0.01 M HC and 0.1 M CTAB, and (d) 0.05 M HC and 0.1 M CTAB in D_2O. The signals of aromatic protons of HC are amplified.

micelle surface. OH^- approaches the CTAB positive charge and promotes HC neutralization. Therefore, even if the quaternary ammonium group cannot be neutralized, the overall charge at the micelle surface diminishes. This also helps the insertion of CAT16 (and CTAB) into the micelles. Such a charge variation may be also related to a structural variation of the aggregates. Due to the interactions between the surfactant heads and the OH^- groups at the micelle surface, the interactions (measured by τ) become stronger, and the environmental micropolarity (measured by $\langle A \rangle$ for the interacting component) increases by adding NaOH. In the presence of HC, the OH^- ions act to neutralize the acidic OH groups of HC and increase the strength of interaction with the surfactant heads in vicinity of HC charged heads. Consequently, the negatively charged groups of HC become more localized at the micelle surface and are neutralized by the positively charged surfactant heads close to them. The surface charge decreases, but the percentage of free CAT16 increases with the increase in HC also in the presence of NaOH, because high concentrations of HC create a barrier to the internalization of the surfactants even in ionized form: indeed the stronger interactions at the micelle surface make the micelles less permeable to the insertion of other surfactants. In this case too, a sketch of the proposed organization of the mixed micelles of CTAB and HC surfactants after neutralization with NaOH is shown in Figure 4c.

The lecithin aggregates show poor variations of the EPR line shape in the different experimental conditions using CAT16 as a probe. This effect is expected due to the close packing of the liposomes (high density of lecithin molecules in the liposomes).

Since the EPR analysis showed interesting information about reproducible structural variations of CTAB micelles upon addition of HC up to a concentration of 0.05 M, we decided to more deeply investigate the structural features of this system using the NMR technique.

3.2. ^{1}H NMR Analysis. The solubilization sites in the micellar system can be determined by using ^{1}H NMR spectroscopy. NMR chemical shifts depend on the molecular environment of the nuclei. Changes in the chemical shifts of surfactants as a function of solubilizate concentration provide precise information on the location of the solubilizate with respect to micelle nuclei. Solubilization of a solute in hydrophobic environment causes a shift to lower frequencies compared to a hydrophilic environment. This allows a differentiation in whether a solute is solubilized in the more hydrophilic or hydrophobic layer.

The 1D ^{1}H NMR spectrum of 0.1 M of CTAB in D_2O, moving from downfield to upfield, shows in sequence: the α-CH_2 multiplet at δ = 3.470 ppm, the largest narrow $^+N(CH_3)_3$ (headgroup) singlet at δ = 3.209 ppm, the broad hump signal of the β-CH_2 at δ = 1.797, the γ-$(CH_2)_2$ signal at δ = 1.396 ppm, the ε-$(CH_2)_{11}$ methylene groups of the alkyl chain at δ = 1.311 ppm and, finally, the triplet of the ω-CH_3 signal at δ = 0.887 ppm.

When HC is added to the CTAB solution, chemical shift variations for CTAB and aromatic-HC protons occurred.

Figure 5 shows ^{1}H NMR spectra for aqueous CTAB (0.1 M) solutions containing different HC concentrations: (a) no HC; (b) 0.005 M HC; (c): 0.01 M HC; (d) 0.05 M HC. Table S1 (SI) summarizes the chemical shifts (δ) of CTAB (a) and aromatic-HC (b) protons, at different HC concentrations.

By increasing HC concentration, the peaks of aromatic-HC and CTAB protons shift to higher magnetic field with the exception of ε-$(CH_2)_{11}$ and ω-CH_3 CTAB protons which show downfield shifts.

At HC concentration of 0.05 M, CTAB chemical shifts are largely perturbed and peak broadening also occurs. In fact, the α-(CH_2), β-(CH_2) and γ-$(CH_2)_2$ signals as well as the ^+N-$(CH_3)_3$ signal, shift to lower values (upfield), with the γ-$(CH_2)_2$ signal shifting under the resonance of the long aliphatic chain. As previously reported,[30−32] this upfield shift is due to ring current shift effects caused by the aromatic portion of HC which is located in the outer micelle part, close to the hydrophilic headgroup of CTAB. At higher HC concentration, the positive shift of the β-CH_2 signal increases. This means that HC is able to penetrate not only the headgroup region but also the palisade layer, in agreement with the EPR results as also sketched in Figure 4a,b. Conversely, the resonance signals of ε-$(CH_2)_{11}$ and ω-CH_3 remain downfield shifts by adding HC. Moreover, because of the nonpolarity of the aromatic ring with its *meta*-alkyl chain, the micelle interior becomes less polar. HC molecules penetrating deeper into CTAB micelles make the nearest surfactant tails move apart (Figure 4b); this is in good agreement with the explanation of Chaghi et al.[31]

dx.doi.org/10.1021/la402008n | *Langmuir* 2013, 29, 11118−11126

Table 2. Chemical Shift (δ, ppm; accuracy ±0.001) Observed for HC 0.01 M and CTAB 0.1 M at Different pH

(a) CTAB Protons

NaOH[M]	pH	α-CH_2	$^+N(CH_3)_3$	β-CH_2	γ-$(CH_2)_2$	ε-$(CH_2)_{11}$	ϕ-CH_3
0	7.6	3.448	3.203	1.767	1.360	1.311	0.901
0.002	8.8	3.444	3.208	1.763	1.331	1.331	0.923
0.012	9.87	3.391	3.165	1.730	1.324	1.324	0.905

(b) HC Aromatic Protons

NaOH[M]	pH	H2	H6	H4	H5
0	7.6	6.629	6.601	6.945	7.151
0.002	8.8	6.598	6.507	6.824	7.106
0.012	9.87	6.382	6.207	6.430	6.942

As shown in Figure 5 and Table S1, by increasing HC concentration, the resonances of its aromatic protons, mainly at the 2- and 5-positions, are more and more shifted upfield. Meanwhile, the two *ortho* protons merge into one peak and all peaks become broad. This is nicely explained by a deeper penetration of HC into CTAB micelles (Figure 4b), so that the aromatic protons in the 2- and 5-positions are the most affected by the less polar environment. Such a penetration is well accounted for by the occurrence of both hydrophobic interactions at the chain level and hydrophilic interactions between HC and CTAB heads, in agreement with the EPR results.

HC is an amphiphilic molecule. Therefore it is oriented in the micelle with the hydroxyl group in the region of the headgroup, whereas the *meta* alkyl chain is inserted in the hydrophobic region (Figure 4a). Likely, the results in Figure 5 and Tables S1 and 2 show that, at the higher concentrations, HC penetrates deeper into the micelle (Figure 4b).[33,34] The line broadening at higher concentration of HC is accompanied by an increase of the viscosity caused by a sphere-to-rod transition of the micelle, in agreement with our EPR results.

Another interesting effect of increasing HC concentration is the peak upfield shift for the aromatic protons. The chemical shift variation follows the trend H2 ≥ H5 > H6 ≥ H4. This variation indicates the bending of the HC head toward the CTAB heads (Figure 4b), which helped the formation of rod-like micellar structures. The subsequent barrier effect of the highly packed micellar structure (high density of surfactants in the micelles) impeded the internalization of external surfactants. This finding is in perfect agreement with the EPR analysis.

These results are also in agreement with those found by other authors[33,34] concerning the solubilization of aromatic compounds in cationic micelles: the highly polar solutes tend to solubilize close to the micelle surface due to ion/polar interactions between the organic solute and micelles. Indeed, HC phenolic −OH partially ionizes in aqueous solution.

To assess the impact of the HC ionization state on the interaction with CTAB micelle, ^{1}H NMR spectra are recorded varying pH from the initial one (pH= 7. 6) by adding sodium hydroxide at different concentrations (0.002 M, 0.012 M) to a solution containing HC 0.01M, and CTAB 0.1M.

The chemical shift (δ) of CTAB protons at different NaOH concentrations are reported in Table 2a.

From the data in Table 2a, it resulted that $^+N(CH_3)_3$, α-(CH_2), β-(CH_2), and γ-$(CH_2)_2$ shift to lower values (upfield), while γ-$(CH_2)_2$ and ω-CH_3 signals shift to higher values (downfield). Furthermore, it was observed that γ-$(CH_2)_2$ and ε-$(CH_2)_{11}$ signals merged into one unresolved peak. This is due to the neutralization reaction between NaOH and HC to produce $C_{21}H_{36}O^-$. This reaction induces a major solubilization of HC in CTAB micelle with the hydrophobic chain penetrating into the palisade layer and the negatively charged head interacting with the positively charged CTAB head, as already hypothesized on the basis of the EPR results (Figure 4c). Furthermore, in the presence of NaOH, the concentration of ions (like Na^+ and Br^-) increases. As a consequence, both the critical micelle concentration (CMC) of surfactant and the volume of micelle increases and probably the shape of CTAB micelle changes toward a rod-like structure. This also justifies the variation of mobility of the surfactant spin probe tested by the EPR analysis.

It may be surprising that the upfield chemical shifts observed for the aromatic protons of HC by increasing the pH of the solution (Table 2b) show a trend for the chemical shift variation of H4 > H6 > H2 > H5, which is opposite to that found by increasing HC concentration (H2 ≥ H5 > H6 ≥ H4). As suggested by the EPR results, this behavior is well explained by the internalization of the HC chain in proximity of the CTAB chain due to the contemporaneous interactions of OH^- and $C_{21}H_{36}O^-$ anions with CTAB heads, which swallows the micellar surface (Figure 4c).

4. CONCLUSIONS

The computer-aided analysis of the EPR spectra of 5DSA and CAT16 spin probes, combined with ^{1}H NMR analysis of the chemical shifts for HC−CTAB water solutions by changing the HC content and the pH of the solution provided detailed information on the structure and organization of the HC−CTAB mixed micelles. The main information is summarized as follows:

- HC added at the lower concentrations (0.005−0.01 M) modifies the structure of the aggregates and originates a more compact, even if not well ordered, structure. Such variations are ascribed to the formation of mixed CTAB/HC micellar aggregates with a "rod-like" shape due to (1) the different sizes of HC and CTAB; and (2) the interactions occurring at the polar surface between CTAB and HC heads. The EPR analysis indicates a lowering in the environmental polarity of the aromatic protons at positions 5 and 4, as supported by the NMR results.
- HC at the higher concentrations creates a mixed-micellar structure that works as a barrier impeding the internalization of free surfactants. Both EPR and NMR results indicate that HC molecules at the higher concentrations penetrate deeper into CTAB micelle so that the aromatic protons in 2- and 5-position are the most affected by a less polar environment. In these conditions, HC deeper internalization promotes the approaching of the positively charged CTAB to the OH groups of HC.

dx.doi.org/10.1021/la402008n | Langmuir 2013, 29, 11118−11126

As a consequence, the surfactant structure is less packed (a lower surfactant density in the micelles) due to the steric hindrance of the aromatic group into the aggregates, close to the external interface. The HC penetration is well accounted for by the occurrence of both hydrophobic interactions at the chain and aromatic group levels, and hydrophilic interactions between the HC and CTAB heads.

- The rise in pH after addition of NaOH increases the surfactant solubility into the micelles in the absence of HC, due to charge neutralization of the CTAB heads. In the presence of HC, the OH^- ions are used to neutralize both the acidic OH groups of HC and, partly, the charge of the CTAB heads. Consequently, the negatively charged ionized HC, which are localized at the micelle surface, interact electrostatically with the positively charged surfactant heads close to them. The surface potential decreases, but, at high concentration, HC still creates a barrier to the internalization of the surfactants due to the stronger localized interactions at the micelle surface and a significant structural perturbation effect monitored by both EPR and NMR.

Lecithin liposomes were also affected by HC in the interactions occurring between the surfactants in the liposomes after HC internalization. However, the close packing of these structures prevented an exhaustive analysis by means of the magnetic resonance techniques.

■ ASSOCIATED CONTENT

Supporting Information

Chemical shift at different HC concentrations (CTAB 0.1M). Experimental and computed EPR spectra of Egg Yolk Lecithin liposomes containing different amounts of HC, and 5DSA as a spin probe; "interacting" components spectra of CAT16 in HC/CTAB micellar solutions at different pH. This material is available free of charge via the Internet at http://pubs.acs.org.

■ AUTHOR INFORMATION

Corresponding Author

*(M.F.O.) Address: DiSTeVA, Loc. Crocicchia, 61029, Urbino, Italy; Tel.: +390722304320; e-mail: maria.ottaviani@uniurb.it. (S.S.) Address: Dip. Sci. Biomol., Via Maggetti 24, 61029 Urbino, Italy; Tel.: +390722303445; e-mail: stefania.santeusanio@uniurb.it.

Notes

The authors declare no competing financial interest.

■ ACKNOWLEDGMENTS

MFO thanks PRIN2012-NANOMed for financial support. COST Action MP1202 is also acknowledged.

■ REFERENCES

(1) John, G.; Shankar, B. V.; Jadhav, S. R.; Vemula, P. K. Biorefinery: A design tool for molecular gelators. *Langmuir* **2010**, *26*, 17843−53.

(2) John, G.; Vemula, P. K. Design and development of soft nanomaterials from biobasedamphiphiles. *Soft Matter* **2006**, *2*, 909−914.

(3) Attanasi, O. A.; Filippone, P. Cardanolo: Una preziosa materia prima rinnovabile. *Chim. Ind. (Milan)* **2003**, *85*, 11−2.

(4) Lomonaco, D.; Santiago, G. M. P.; Ferreira, Y. S.; Arriaga, A. M. C.; Mazzetto, S. E.; Mele, G.; Vasapollo, G. Study of technical CNSL and its main components as new green larvicides. *Green Chem.* **2009**, *11*, 31−33.

(5) Balachandran, V: S.; Jadhav, S. R.; Vemula, P. K.; John, G. Recent advances in cardanol chemistry in a nutshell: From a nut to nanomaterials. *Chem. Soc. Rev.* **2013**, *42* (2), 427−38 and references cited therein..

(6) Suresh, K. I.; Kishanprasad, V. S. Synthesis, structure, and properties of novel polyols from cardanoland developed polyurethanes. *Ind. Eng. Chem. Res.* **2005**, *44*, 4504−4512.

(7) Himejima, M.; Kubo, I. Antibacterial agents from the cashew *Anacardium occidentale* (Anacardiacae) nut shell oil. *J. Agric. Food Chem.* **1991**, *39*, 418−421.

(8) Paramashivappa, R.; Kumar, P. P.; Vithayathil, P. J.; Rao, A. S. Novel method for isolation of major phenolic constituents from cashew (*Anacardium occidentale*) nut shell liquid. *J. Agric. Food Chem.* **2001**, *49*, 2548−51.

(9) Subbarao, C. N.; Krishna, K. M.; Prasad, V. S. Review on applications, extraction, isolation and analysis of cashew nut shell liquid (CNSL). *Pharma Res. J.* **2011**, *6*, 21−25.

(10) Kozubek, A.; Tyman, H. H. P. Resorcinolic lipids, the natural non-isoprenoid phenolic amphiphiles and their biological activity. *Chem. Rev.* **1999**, *99*, 1−26.

(11) John, G.; Masuda, M.; Ohada, Y.; Yase, K.; Shimizu, T. Nanotube formation from renewable resources via coiled nanofibers. *Adv. Mater.* **2001**, *13*, 715−18.

(12) Scott, G. Degradable Polymers: Principles and Applications; Springer: Berlin, 2003; p 192.

(13) Balachandran, V: S.; Jadhav, S. R.; Pradhan, P.; De Carlo, S.; John, G. Adhesive vesicles through adaptive response of a biobased surfactant. *Angew. Chem., Int. Ed.* **2010**, *49*, 9509−12.

(14) Nakatsu, T.; Chen, Z. U.S. Patent No. 07/685, 285, 15.05, 1991.

(15) Amorati, R.; Pedulli, G. F.; Valgimigli, L.; Attanasi, O. A.; Filippone, P.; Fiorucci, C.; Saladino, R. Absolute rate constants for the reaction of peroxyl radicals with cardanol derivatives. *J. Chem. Soc., Perkin Trans. 2* **2001**, 2142−46.

(16) Attanasi, O. A.; Berretta, S.; Favi, G.; Filippone, P.; Mele, G.; Moscatelli, G.; Saladino, R. Tetrabromo hydrogenated cardanol: Efficient and renewable brominating agent. *Org. Lett.* **2006**, *8*, 4291−93.

(17) Rangel-Yagui, O. C.; Pessoa, A.; Tavares, L. C. Micellar solubilization of drugs. *J. Pharm. Pharm. Sci.* **2005**, *8*, 147−63.

(18) Chu, W. Remediation of contaminated soils by surfactant-aided soil washing. *Pract. Period. Hazard., Toxic, Radioact. Waste Manage.* **2003**, *7*, 19−24.

(19) Ottaviani, M. F.; Moscatelli, A.; Desplantier-Giscard, D.; Di Renzo, F.; Kooyman, P. J.; Alonso, B.; Galarneau, A. Synthesis of micelle-templated silicas from cetyltrimethylammonium bromide/1,3,5-trimethylbenzene micelles. *J. Phys. Chem. B* **2004**, *108*, 12123−29.

(20) Ottaviani, M. F.; Baglioni, P.; Martini, G. Micellar solutions of sulfate surfactants studied by electron spin resonance of nitroxide radicals. 1. Use of neutral and positively charged spin probes. *J. Phys. Chem.* **1983**, *87*, 3146−53.

(21) Baglioni, P.; Rivara-Minten, E.; Dei, L.; Ferroni, E. ESR study of sodium dodecyl sulfate and dodecyltrimethylammoium bromide micellar solutions. Effect of urea. *J. Phys. Chem.* **1990**, *94*, 8218−8222.

(22) Levstein, P. R.; van Willigen, H. Photoinduced electron transfer from porphyrins to quinones in micellar systems: An FT-EPR study. *Chem. Phys. Lett.* **1991**, *187*, 415−422.

(23) Brigati, G.; Franchi, P.; Lucarini, M.; Pedulli, G. F.; Valgimigli, L. The EPR study of dialkyl nitroxides as probes to investigate the exchange of solutes between micellar and water phases. *Res. Chem. Intermed.* **2002**, *28*, 131−141.

(24) Kogan, A.; Rozner, S.; Mehta, S.; Somasundaran, P.; Aserin, A.; Garti, N.; Ottaviani, M. F. Characterization of the nonionic microemulsions by EPR. I. Effect of solubilized drug on nanostructure. *J. Phys. Chem. B* **2009**, *113*, 691−699.

(25) Ottaviani, M. F.; Favuzza, P.; Sacchi, B.; Turro, N. J.; Jockusch, S.; Tomalia, D. A. Interactions between starburst dendrimers and mixed DMPC/DMPA-Na vesicles studied by the spin label and the spin probe techniques, supported by TEM. *Langmuir* **2002**, *18*, 2347−57.

(26) Deo, P.; Deo, N.; Somasundaran, P.; Moscatelli, A.; Jockusch, S.; Turro, N. J.; Ananthapadmanabhan, K. P.; Ottaviani, M. F. Interactions of a hydrophobically modified polymer with oppositely charged surfactants. *Langmuir* **2007**, *23*, 5906−13.
(27) Budil, D. E.; Lee, S.; Saxena, S.; Freed, J. H. Nonlinear-least-squares analysis of slow-motion EPR spectra in one and two dimensions using a modified Levenberg−Marquardt algorithm. *J. Magn. Reson., Ser. A* **1996**, *120*, 155−89.
(28) Egret-Charlier, M.; Sanson, A.; Ptak, M. Ionization of fatty acids at the lipid−water interface. *FEBS Lett.* **1978**, *89*, 313−6.
(29) Gross, K. C.; Seybold, P. G. Substituent effects on the physical properties and pK_a of phenol. *Int. J. Quantum Chem.* **2001**, *85*, 569−579.
(30) Bunton, C. A.; Cowell, C. P. The binding of phenols and phenoxide ions to cationic micelles. *J. Colloid Interface Sci.* **1988**, *122*, 154−62.
(31) Chaghi, R.; de Ménorval, L.-C.; Charnay, C.; Derrien, C.; Zajac, J. Interactions of phenol with cationic micelles of hexadecyltrimethylammonium bromide studied by titration calorimetry, conductimetry, and ^{1}H NMR in the range of low additive and surfactant concentrations. *J. Colloid Interface Sci.* **2008**, *326*, 227−34.
(32) Sabatino, P.; Szczygiel, A.; Sinnaeve, D.; Hakimhashemi, M.; Saveyn, H.; Martins, J. C.; Van der Meeren, P. NMR study of the influence of pH on phenol sorption in cationic CTAB micellar solutions. *Colloids. Surf. A* **2010**, *370*, 42−8.
(33) Xu, K.; Ren, H.; Zeng, G.; Ding, L.; Huang, J. Investigation of interaction between phenol and cetylpyridinium chloride micelle in the absence and in the presence of electrolyte by ^{1}H NMR spectroscopy. *Colloids. Surf. A* **2010**, *356*, 150−55.
(34) Heins, A.; Sokolowski, T.; Stöckmann, H.; Schwarz, K. Investigating tha location of propyl gallate at surfaces and its chemical microenvironment by ^{1}H NMR. *Lipids* **2007**, *42*, 561−72.